coatings

MDPI

Article

The Antibacterial Properties of a Silver Multilayer Coating for the Prevention of Bacterial Biofilm Formation on Orthopedic Implants—An In Vitro Study

Sanne W. G. van Hoogstraten [1], Janine Fechter [2], Rainer Bargon [2], Julia L. van Agtmaal [1], Laura C. W. Peeters [1], Jan Geurts [1] and Jacobus J. C. Arts [1,3,*]

[1] Laboratory for Experimental Orthopaedics, Department of Orthopaedic Surgery, Care and Public Health Research Institute (CAPHRI), Maastricht University Medical Centre, 6229 Maastricht, The Netherlands; s.vanhoogstraten@maastrichtuniversity.nl (S.W.G.v.H.)
[2] Department of Research and Development, Aesculap AG, Am Aesculap-Platz, 78532 Tuttlingen, Germany; janine.fechter@aesculap.de (J.F.)
[3] Department of Biomedical Engineering, Orthopaedic Biomechanics, Eindhoven University of Technology, 5612 Eindhoven, The Netherlands
* Correspondence: j.arts@mumc.nl

Abstract: The prevention of biofilm formation on orthopedic implants is essential, as biofilms are the main challenge in the effective treatment of periprosthetic joint infection (PJI). A silver multilayer (SML) coating was developed to prevent biofilm formation on the implant surface. Previous studies have already demonstrated its antibacterial properties without cytotoxic effects. However, the coating has not been previously tested when applied to common titanium surfaces used in total joint arthroplasty implants. These surfaces often have increased roughness and porosity in the case of cementless implants, which can alter the antibacterial effect of the coating. In this study, we assessed the antibacterial and anti-biofilm properties of the SML coating on corundum-blasted and plasma-sprayed microporous-coated titanium alloy surfaces, using *S. aureus*, *S. epidermidis*, and *E. coli*. An antibacterial activity test following the principles of ISO 22196, ASTM E2180-18, and JIS Z 2801 standards was performed, as well as a biofilm proliferation assay investigating bacterial adhesion and biofilm formation. The SML coating exhibited strong antibacterial effects for all bacterial strains. After 24 h biofilm culture, a >4-log reduction in CFU was induced by the SML coating for *S. epidermidis* and *E. coli* on the corundum-blasted and plasma-sprayed microporous-coated titanium surfaces, respectively, when compared to the uncoated surfaces. The coating showed bactericidal properties against Gram-positive bacteria on the corundum-blasted discs. The SML coating on two common titanium surfaces demonstrates significant potential as an effective strategy in combating PJI across a wide range of orthopedic implants.

Keywords: prosthetic joint infections; biofilm formation; in vitro; antibacterial coating; silver

Citation: van Hoogstraten, S.W.G.; Fechter, J.; Bargon, R.; van Agtmaal, J.L.; Peeters, L.C.W.; Geurts, J.; Arts, J.J.C. The Antibacterial Properties of a Silver Multilayer Coating for the Prevention of Bacterial Biofilm Formation on Orthopedic Implants—An In Vitro Study. *Coatings* **2024**, *14*, 216. https://doi.org/10.3390/coatings14020216

Academic Editor: Peter Zilm

Received: 22 December 2023
Revised: 26 January 2024
Accepted: 30 January 2024
Published: 9 February 2024

1. Introduction

Periprosthetic joint infection (PJI) is a severe complication that can occur after joint replacement surgery, leading to significant patient suffering, morbidity, and healthcare costs. With a 5-year mortality rate of >21%, PJI is a major problem in orthopedic surgery [1]. The incidence of PJI is estimated to be 1%–2% after primary surgery [2–7]. In hip and knee arthroplasty surgery, PJI is the main cause of 15% and 25% of all revisions, respectively [8–11]. As more than a million primary total hip arthroplasties are performed annually worldwide, the prevalence of PJI is extremely high and is expected to keep rising due to the growing target population for total joint arthroplasty [12–15]. Also, the rapid emergence of antimicrobial resistance (AMR) endangers the efficacy of antibiotic treatment strategies for PJI [16,17].

PJI treatment is complex and consists of antibiotic therapy and surgery, where the main surgical options are debridement and retention of the implant, particularly for early

infections, and resection arthroplasty with re-implantation in one or two stages [18–20]. The failure rate of PJI treatment is high (10%–45%), mainly attributed to the formation of bacterial biofilms [21,22]. Biofilm formation is a multi-stage process, where bacteria adhere to the implant surface, cluster together to form microcolonies, and produce an extracellular matrix (ECM) [23]. The ECM shields the bacteria against host immune cells as well as antibiotics, and the efficacy of antibiotic treatment decreases as bacteria within the biofilm can have a lower metabolic rate [24]. With implant-retaining surgical debridement, it is challenging to remove all biofilm from the implant without creating excessive side damage to the implant or healthy tissue. Also, mature biofilms release daughter cells, leading to new infection loci on the implant or elsewhere in the body with hematogeneous spread [25]. The rapid emergence of resistant bacteria increasingly endangers the range of effective antibiotic therapies, as the main pathogens involved in PJI are *Staphylococcus aureus* and coagulase-negative staphylococci, predominantly *Staphylococcus epidermidis*, with increasing incidence of MRSA infections [16,26–28]. Surviving bacteria within the biofilm after PJI treatment are the main cause of PJI recurrence [29]. Therefore, there is a critical need for preventative strategies for biofilm formation on orthopedic implants. Additional solutions that protect implant surfaces against biofilm formation, not depending solely on antibiotics, should be developed and implemented in clinical practice.

Various antibacterial implant coatings not based on antibiotics are available in the clinic, mostly based on silver as an antimicrobial agent [30]. Silver is an effective antimicrobial compound, whereby free silver ions interfere with bacterial energy production, impair the integrity of the bacterial cell wall, and bind to cellular components, thereby interfering with cellular processes [31]. However, challenges are present when using silver in an antimicrobial implant coating, as the strength of the antibacterial properties and safety levels must be balanced by the silver concentration [32]. With high silver concentrations, toxic side effects such as argyria can occur, while low concentrations yield limited antibacterial efficacy [33,34]. So far, a few silver-based antimicrobial coatings have been implemented in the clinic, such as the MUTARS® tumor prosthesis and the AgPROTEX® coating on total hip arthroplasty implants. However, the use of the current antimicrobial-coated implants is only justified in high-risk cases after individual risk–benefit analysis, as there is a lack of prospective randomized clinical trials [35]. Also, the available antimicrobial implant coatings are only suitable for metal implants and cannot be applied to polymer surfaces, while polyethylene liners are highly susceptible to biofilm formation [36].

A silver multilayer coating (SML) (HyProtect™, Bio-Gate, Nuernberg, Germany) has been developed in previous studies, which consists of an ultra-thin layer containing silver clusters embedded in a polysiloxane (SiO_xC_y) matrix [37,38]. This coating can be applied to metal as well as polymer components. The SML coating has been characterized in previous studies, as described by Fabritius et al., whereby the chemical structure, silver content, and coating thickness were analyzed [37]. Because of the thinness of the coating (~90 nm), the surface structure of the substrate material is not affected. An SEM image of the cross-section of the coating is shown in Supplementary Figure S1. The safety and antibacterial properties of the SML coating have been shown in multiple studies, which include in vitro, in vivo and ex vivo antimicrobial activity assays, as well as in vitro and in vivo cytotoxicity assays [37–40]. Also, a clinical case study was performed where the SML coating was used in a knee arthrodesis after recurrent prosthetic knee infection, and silver blood concentrations after 48 h remained under the detection limit of 2 ppb [41].

The SML coating is a high-potential antibacterial coating; however, it is widely known that the susceptibility of bacterial adhesion to implant surfaces and the efficacy of an antibacterial coating depends on the surface properties of the implant and the pathogenic microorganisms involved. Surface roughness and porosity can affect the coating surface area as well as the susceptibility to the adherence of bacteria [42]. Importantly, orthopedic implants often have significantly higher roughness to promote bone ingrowth, especially cementless implants where the base surface is often sputter-coated to increase roughness. The antibacterial properties of the SML coating on these substrate materials have not

been assessed. In addition, little is known about the antibacterial mechanism of the coating and the effect of the coating in different phases of biofilm formation, including bacterial adhesion, biofilm formation and maturation, and biofilm dispersal. Therefore, the objectives of this study were to assess the antibacterial properties of the SML coating on two titanium substrate materials broadly applied in total joint replacement and to elucidate the antibacterial mechanism of the SML coating using different in vitro models following the principles of the ISO 22196, ASTM E2180-18, and JIS Z 2801 testing standards.

2. Materials and Methods

2.1. Test Samples

Two types of titanium discs (Ø14 mm × 5 mm) with different roughness values were used as base materials for the coating. Corundum-blasted (CB) and plasma-sprayed microporous-coated (PS) titanium discs were included as substrate materials for the SML coating. The CB discs had a roughness of Ra 3.5–5.5 µm, and the PS discs (with the base material Ti6Al4V according to ISO 5832-3 and coated with commercially pure titanium according to ISO 5832-2; Plasmapore®, Aesculap AG, Tuttlingen, Germany) had a pore size ranging from 50 to 200 µm with a microporosity of 35%. These test items were coated with the SML coating [37,38,41]. Firstly, a SiO_xC_y base layer was deposited on the respective surface by means of chemical vapor deposition (CVD), after which silver clusters (~2.7 µg/cm^2, as measured by ICP-OES) were deposited on the base layer by means of physical vapor deposition (PVD). Thirdly, a top layer of SiO_xC_y was applied by means of CVD, resulting in a coating with a thickness of ~90 nm, as measured using spectral ellipsometry. The coated items were packed individually, and gamma sterilized (BBF Sterilisationsservice GmbH, Kernen-Rommelshausen, Germany). The two experimental groups included in this study are non-SML-coated (referred to as 'uncoated') and SML-coated discs. Uncoated CB, SML-coated CB, uncoated PS, and SML-coated PS titanium discs were included as experimental groups in all experiments in this study. The materials are shown in Supplementary Figure S2.

2.2. Bacterial Culture

Staphylococcus aureus ATCC 6538P, *S. epidermidis* ATCC 35984, and *Escherichia coli* ATCC 8739 were used to assess the antibacterial and anti-biofilm properties of the SML coating. Bacterial stocks were stored in 20% glycerol at −80 °C. The strains were inoculated onto blood agar plates and incubated overnight under aerobic conditions at 37 °C. The bacteria were cultured in 5 mL tryptic soy broth (TSB; Sigma-Aldrich, St Louis, MO, USA, 22092) for 18 h at 37 °C at 200 rpm, washed with PBS, and diluted to the target inoculum concentration based on the optical density at 600 nm in the desired solution as will be discussed below.

2.3. Antibacterial Activity Test

The antibacterial activity of the SML coating on CB discs was examined according to the principles of the ISO 22196, ASTM E2180-18, and JIS Z 2801 test standards [43,44]. The antibacterial activity of the SML coating on the PS discs was not tested according to these standards due to the porosity of the surfaces. In each experiment, six uncoated discs and three SML-coated discs were included, and for each bacterial strain, the experiment was performed in triplicate. A molten agar slurry was made by diluting nutrient broth (NB; Sigma-Aldrich, 70149) 500× with sterile DI water and adding 0.9 gr of agar (Sigma-Aldrich, 05040) per 300 mL of the diluted NB. The pH value of this molten agar slurry was adjusted to 7.0 through the addition of sodium hydroxide or hydrochloric acid. All reagents used in the experiments in this study were high-pressure steam-sterilized at 121 °C for 15 min. The test inoculum with a target concentration of 6×10^5 colony-forming units (CFUs)/mL was prepared by diluting the bacterial culture in the molten agar slurry (45 °C). The test discs were aseptically placed on a 12-well sterile polystyrene tissue culture plate and were pre-wetted with sterile saline. All discs were inoculated with 100 µL of the test inoculum, with the inoculum homogeneously spread across the sample surface. According to the ISO 22196 standard, three uncoated discs were retrieved directly after inoculation and

processed for CFU counting, to determine the starting inoculum level in the agar slurry on each sample. The discs were placed in 5 mL neutralizing broth (casein peptone lecithin polysorbate broth, Sigma-Aldrich, 22089; Tween-20, Sigma-Aldrich, P7949), and bacteria were detached from the discs by means of 10 min sonication in a sonication bath (Branson 2210 sonicator, Branson Ultrasonics Co., Ltd, Danbury, CT, USA) and 5 s vortexing [43–46]. The viable bacteria retrieved from each sample were quantified by making a serial dilution of the sonicate and plating out 100 µL aliquots of the serial dilution on blood agar plates in duplo (Thermo Scientific, Waltham, MA, USA, R01217). After 24 h incubation of the plates at 37 °C, the CFUs were counted. The remaining uncoated discs (n = 3) and SML-coated discs (n = 3) were incubated for 24 h at 37 °C in a humid environment. After the incubation period, the discs were processed for CFU counting as described above. The log reduction in CFUs between the uncoated discs and the SML-coated discs was calculated, and the antibacterial activity (R) was calculated using the following formula:

$$R = U_t - A_t \quad (1)$$

where U_t and A_t are the average of the decadic logarithm of the number of viable bacteria recovered from the uncoated and SML-coated test discs, respectively. Also, the percentage of reduction in CFU on the discs when comparing the uncoated and SML-coated discs was calculated as:

$$\%\text{reduction} = \frac{\text{CFU(uncoated)} - \text{CFU(SML-coated)}}{\text{CFU(uncoated)}} \times 100 \quad (2)$$

where CFU(uncoated) and CFU(SML-coated) are the average number of CFUs on the uncoated and SML-coated test discs, respectively.

2.4. Biofilm Proliferation Assay

A biofilm proliferation assay was performed to investigate the antibacterial properties of the SML coating on both CB and PS discs as compared to uncoated discs. For each bacterial strain, all experiments were performed in triplicate. Different stages of biofilm formation were investigated, including bacterial adhesion, biofilm maturation, and daughter cell dispersal, as will be described below. The test inoculum with a concentration of 10^6 CFU/mL was prepared by diluting the bacterial culture in TSB. The test discs were aseptically placed in 24-well sterile polystyrene tissue culture plates and pre-wetted with sterile saline. All discs were inoculated with 1 mL of the test inoculum and were incubated for 1 h at 37 °C in a humid environment.

2.4.1. Effect of the SML Coating on Bacterial Adhesion

After 1 h, a part of the discs was retrieved for CFU counting (n = 3 per group), to determine the anti-adhesion properties of the coating. The discs were rinsed with PBS and placed in 5 mL PBS, and the bacteria were detached from the discs following 5 min of sonication in a sonication bath and 5 s of vortexing. The viable bacteria retrieved from each sample were quantified by making a serial dilution of the sonicate and plating out 100 µL aliquots of the serial dilution on blood agar plates. After 24 h incubation of the blood agar plates at 37 °C, the CFUs were counted. The log reduction in CFUs between the uncoated discs and the SML-coated discs after 1 h of bacterial exposure was calculated as a measure of their adhesion.

2.4.2. Effect of the SML Coating on Biofilm Formation and Maturation

The remaining discs that were not retrieved for CFU counting after 1 h of incubation were washed in PBS to remove non-adherent cells. Fresh 1% TSB (1 mL) was added to each sample, and the discs were incubated for 24 h at 37 °C in a humid environment to form a biofilm. After 24 h, the effect of the SML coating on biofilm maturation was assessed using three read-outs.

Firstly, the discs were processed for CFU counting (n = 3 per group) as described above. The bacteriostatic and bactericidal properties of the SML coating were assessed by looking at whether further growth of adherent bacteria is prevented in the biofilm formation stage or whether adherent bacteria are actively killed by the SML coating. The suppression of bacterial growth shows bacteriostatic properties, whereas the killing of bacteria shows bactericidal properties [47].

Secondly, biofilm biomass was quantified with safranin staining (n = 4 per group) [48]. Safranin is a positively charged dye, which adheres to cell membranes and substances in the biofilm matrix, consisting mainly of exopolysaccharides, extracellular DNA (eDNA), and proteins. The biofilms were washed with PBS to remove media residues and fixed with 1 mL of 10% formalin (VWR, Radnor, PA, USA, 2090.368) for 10 min. The biofilms were rinsed three times with 2 mL of Milli-Q to remove all of the fixative. After air-drying for 30 min, the biofilms were stained with 1 mL of 0.5% safranin per well for 10 min. The excess staining was rinsed off with Milli-Q, and the staining adherent to the biomass was solubilized with 33% glacial acetic acid (VWR, 20102.292). Approximately 100 µL of the solubilized staining was pipetted onto a transparent 96-well plate, and four technical replicates per sample were included. The absorbance of the staining extracted from the biofilms was measured at 540 nm in a microplate reader (Multiskan FC, Thermo Scientific). The percentage of reduction in biomass when comparing the uncoated and SML-coated discs was calculated as:

$$\%\text{reduction} = \frac{OD_{540}(\text{uncoated}) - OD_{540}(\text{SML-coated})}{OD_{540}(\text{uncoated})} \times 100 \quad (3)$$

where OD_{540}(uncoated) and OD_{540}(SML-coated) are the average absorbances measured on the uncoated and SML-coated test discs, respectively. As background controls, two discs per experimental group were included that were inoculated with TSB without a bacterial inoculum. The background signals from these discs were subtracted from the experimental data.

Thirdly, biofilm morphology was assessed using scanning electron microscopy (SEM) (n = 2 per group). The biofilms were washed with PBS to remove media residues, and fixed in 2.5% glutaraldehyde (Sigma-Aldrich, G5882) in 0.1 M phosphate buffer for 1 day. After secondary fixation with 1% osmium tetroxide in 0.1 M phosphate buffer, the discs were dehydrated following a graded series of ethanol. After dehydration in ethanol, the discs were chemically dried with hexamethyldisilazane (Sigma-Aldrich, 440191). The discs were mounted to specimen stubs (AGAR scientific, Essex, UK) and sputter-coated with 5 nm carbon (Leica ACE600, Amsterdam, The Netherlands). Biofilms were viewed and imaged using a scanning electron microscope (Jeol JSM-IT200 InTouchScope™, Freising, Germany). SEM images were taken of three different spots on the sample surface. Two discs per experimental group were included that were inoculated with TSB only without a bacterial inoculum.

2.4.3. Effect of the SML Coating on Biofilm Dispersal

The effect of the SML coating on biofilm dispersal was assessed based on the reproduction and release of daughter cells, using Certika test principles [49,50]. After 24 h of biofilm culture, the discs were retrieved for CFU counting as described above, and the remaining media in the wells were supplemented with 1 mL of TSB to cultivate the daughter cells that were dispersed by the biofilm (n = 3 per group). The daughter cells were cultured for 18 h at 37 °C at 200 rpm. After 0, 6, and 24 h of culture, the growth activity of these offspring bacteria was assessed by measuring the optical density of the daughter cell cultures (OD_{600}). Differences in the growth curves between the SML-coated and uncoated discs could indicate a reduction in biofilm formation and/or a lower rate of daughter cell dispersal by the biofilm. A shift in the growth curve at OD_{600} of 6 h when comparing daughter cell cultures obtained from the SML-coated discs and uncoated discs indicates a reduction in proliferated daughter cells of 3-log scales [49].

2.5. Statistics

All data were assumed to be normally distributed. For each test, the uncoated and SML-coated discs with the same base material (CB or PS discs) were compared using an unpaired *t*-test. All statistical analyses were carried out using GraphPad Prism 10.0 (GraphPad Software, Inc., Boston, MA, USA).

3. Results

3.1. Antibacterial Activity Test

The number of viable bacteria in the agar slurry retrieved after 24 h incubation from the uncoated or SML-CB discs is shown in Figure 1. The number of viable bacteria on the SML-coated discs was significantly lower than on the uncoated discs. For *S. aureus* and *S. epidermidis*, a reduction greater than 3 log was found. For *E. coli*, a reduction greater than 2 log was found. The coating showed bactericidal properties against all tested bacterial strains, as bacteria in the starting inoculum were actively killed. Corresponding R-values and the percentage of reduction in CFUs on the test discs induced by the SML coating were calculated for all bacterial strains, as reported in Table 1.

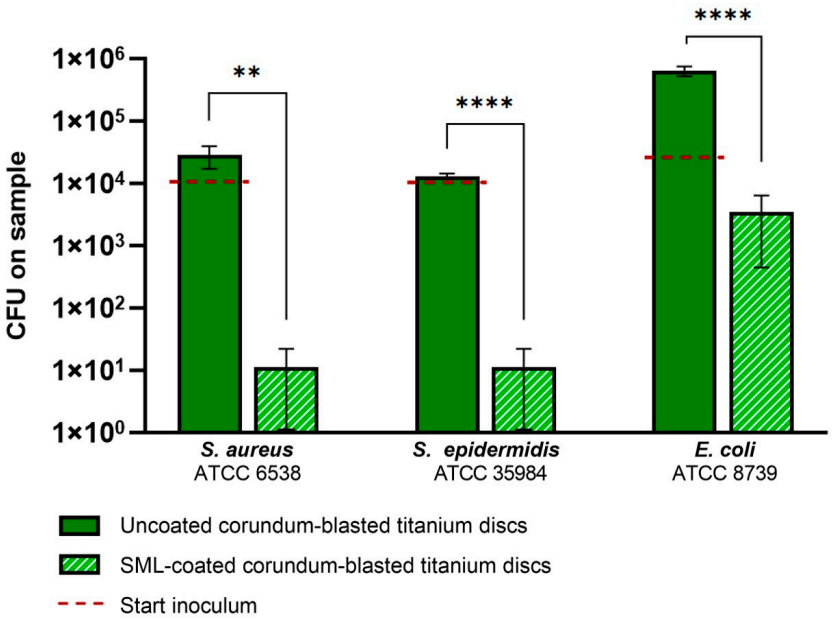

Figure 1. Viable bacteria retrieved from the discs in the antibacterial activity test after 24 h of culture. Uncoated corundum-blasted (CB) titanium discs are represented by dark green bars, and SML-coated CB titanium discs are represented by striped light green bars. The starting inoculum is represented by the red dotted bar. Statistically evaluated with an unpaired *t*-test. ** $p < 0.01$; **** $p < 0.001$. The data represent the average means and standard errors of three separate repeated experiments with triplicate samples for each experimental group.

Table 1. Antibacterial activity R and percentage of reduction in CFUs on the test discs induced by the SML coating (calculated from the antibacterial activity test data).

Bacterial Strain	Antibacterial Activity R	Reduction in CFUs (%)
S. aureus	4.0	>99.9
S. epidermidis	3.7	>99.9
E. coli	2.8	>99.4

3.2. Biofilm Proliferation Test

3.2.1. Effect of the SML Coating on Bacterial Adhesion

Figure 2 shows the number of bacteria that adhered to the surface of the discs after 1 h of incubation. Both CB discs (green bars) and PS discs (orange bars) with and without the SML coating were included. As expected, there was little effect of the SML coating on the number of adherent bacteria after 1 h of incubation. The largest reduction (0.3-log) was observed for *E. coli* adhesion on the PS discs.

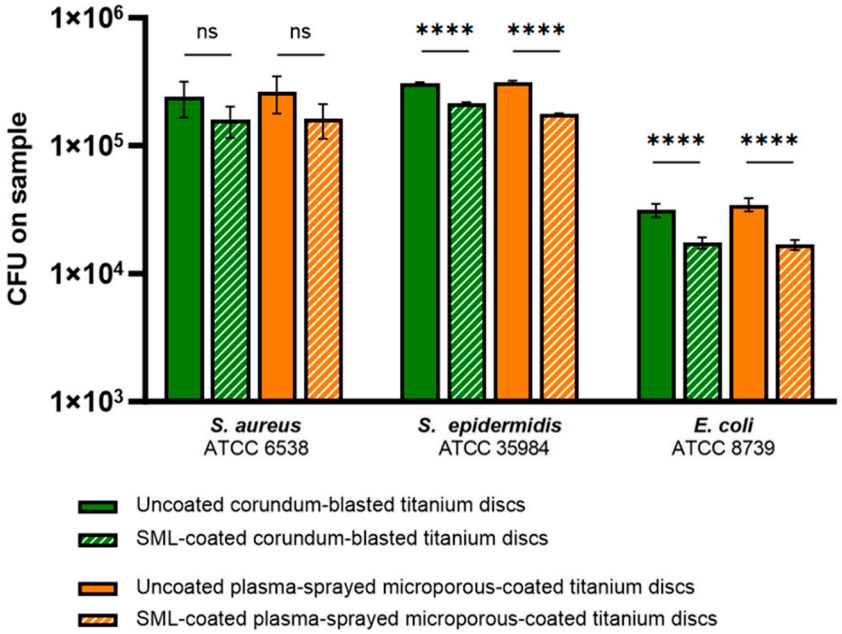

Figure 2. The number of bacteria attached to the sample surface after 1 h of incubation. Green bars represent corundum-blasted (CB) titanium discs and orange bars represent plasma-sprayed microporous-coated (PS) titanium discs. Striped bars show the data of the SML-coated discs. Statistically evaluated with an unpaired *t*-test. ns $p > 0.05$; **** $p < 0.001$. The data represent the average means and standard errors of three separate repeated experiments with triplicate samples for each experimental group.

3.2.2. Effect of the SML Coating on Biofilm Formation and Maturation

CFU Counts

Figure 3 shows the number of viable bacteria within the biofilm after 24 h of biofilm growth. Again, CB discs (green bars) and PS discs (orange bars) with and without the SML coating were included. The SML coating shows a large effect on the number of viable bacteria on the discs. A >4-log reduction in CFUs was found for *S. epidermidis* on the CB discs and *E. coli* on the PS discs. In Table 2, the reductions in viable bacteria on the discs (on the log 10 scale) when comparing the uncoated discs and SML-coated discs can be found.

Table 2. Log reduction in CFUs induced by the SML coating on corundum-blasted and plasma-sprayed microporous-coated titanium discs for all three bacterial strains.

Bacterial Strain	Log_{10} (±SD) Reduction	
	Corundum-Blasted	Plasma-Sprayed Microporous-Coated
S. aureus	3.42 (±0.33)	2.48 (±0.15)
S. epidermidis	4.87 (±0.20)	2.67 (±0.01)
E. coli	2.72 (±0.10)	4.32 (±0.31)

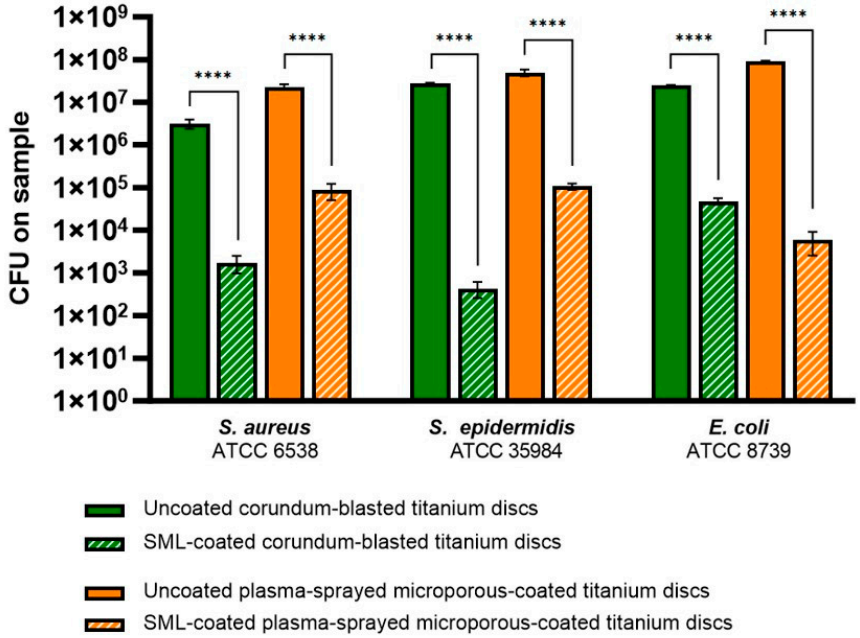

Figure 3. The number of bacteria in the biofilm after 24 h of culture. Again, green bars represent corundum-blasted (CB) titanium discs and orange bars represent plasma-sprayed microporous-coated (PS) titanium discs. Striped bars show the data of the SML-coated discs. Statistically evaluated with an unpaired *t*-test. **** $p < 0.001$. The data represent the average means and standard errors of three separate repeated experiments with triplicate samples for each experimental group.

Bacteriostatic and Bactericidal Properties of the SML Coating

The bacteriostatic and bactericidal properties of the SML coating were assessed by looking at whether the further growth of adherent bacteria is prevented in the biofilm formation stage or whether adherent bacteria are even actively killed by the SML coating. In Figure 4, CB discs (green bars) and PS discs (orange bars) with and without SML coating were included. As can be seen in Figure 4 and as discussed earlier, the bacterial adhesion levels were comparable for the uncoated and SML-coated discs, and the main part of the bacteria in the original starting inoculum adhered to the discs. After further culture of these adherent bacteria in fresh media, the uncoated discs showed an increase in viable bacteria, whereas the SML-coated discs showed suppression of further growth or even active killing of the adherent bacteria. This was observed for all bacterial strains with both CB and PS discs. With the SML coating on the CB discs, a 2-log decrease in CFU was observed for *S. aureus* and *S. epidermidis* when comparing the CFU count after 1 and 24 h of culture. This indicates that adherent bacteria were killed, and the coating thus exerted bactericidal properties. The other groups showed bacteriostatic properties.

Biofilm Biomass Quantification

After biofilm culture, the formed biomass on the discs was quantified with safranin staining. OD_{540} values were obtained and are shown in Figure 5. In all groups, great reductions in biomass were found when comparing the uncoated discs to the SML-coated discs. In Table 3, the percentage of reduction in biomass can be found, when comparing the uncoated and SML-coated discs. On the CB discs, *E. coli* formed significantly lower biofilm than the Gram-positive strains, and the smallest effect of the SML coating on biomass formation was found in this group. However, the largest effect of the coating was found for *E. coli* on the PS discs, with no biomass left on the SML-coated discs. Higher amounts of biomass were detected on the PS discs compared to the CB discs. For the Gram-positive strains, a mean OD_{540} of roughly five times higher was found when comparing the uncoated PS discs to the CB discs. For *E. coli*, the mean OD_{540} was roughly 15 times higher.

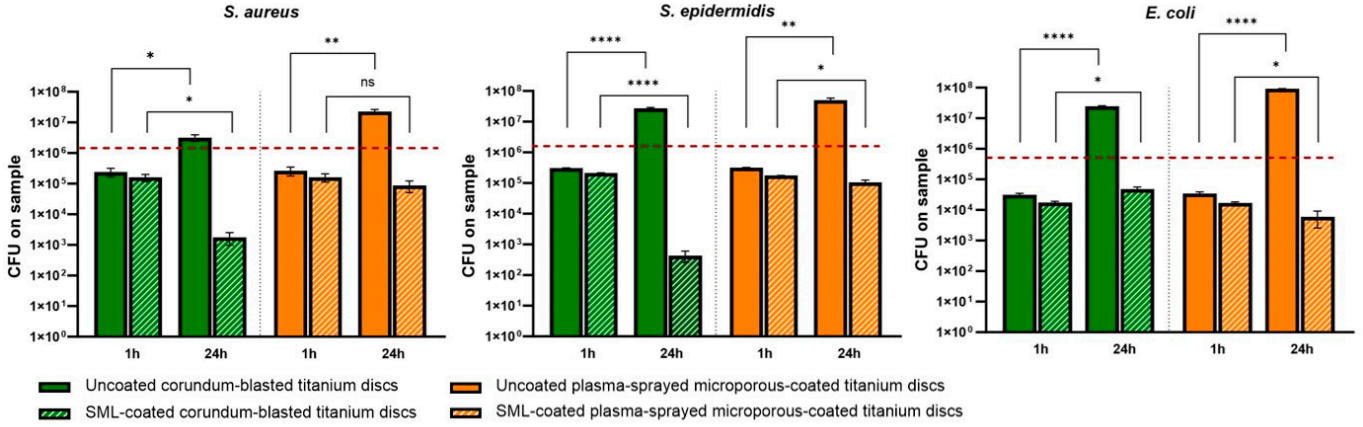

Figure 4. Viable bacteria on the discs after 1 h of bacterial adhesion and 24 h biofilm formation, indicating bacteriostatic or bactericidal coating properties. The red dotted line indicates the starting inoculum level. Green bars represent corundum-blasted (CB) titanium discs and orange bars represent plasma-sprayed microporous-coated (PS) titanium discs. Striped bars show the data of the SML-coated discs. Statistical evaluations between groups indicative of bacteriostatic or bactericidal properties were performed with an unpaired *t*-test. ns $p > 0.05$, * $p < 0.05$, ** $p < 0.01$, and **** $p < 0.001$. The data represent the average means and standard errors of three separate repeated experiments, with quadruplicate samples for each experimental group.

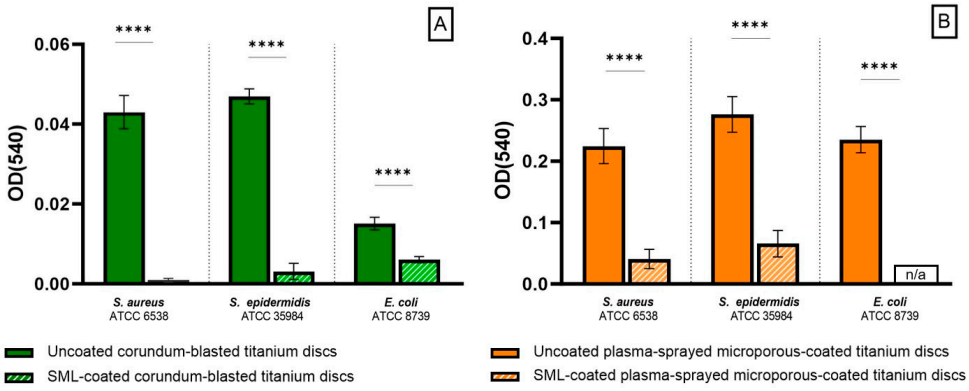

Figure 5. Biofilm biomass assessed by means of safranin staining (OD_{540}) on uncoated and SML-coated (**A**) corundum-blasted (CB) and (**B**) plasma-sprayed microporous-coated (PS) titanium discs, after 24 h of biofilm culture. **** $p < 0.001$. No biomass was found on the SML-coated PS discs inoculated with *E. coli* (n/a). The data represent the average means and standard errors of three separate repeated experiments with triplicate samples for each experimental group.

Table 3. Percentage of reduction in biomass (OD_{540}) induced by the SML coating on corundum-blasted and plasma-sprayed microporous-coated titanium discs, for all three bacterial strains.

Bacterial Strain	Reduction in Biomass (OD_{540})	
	Corundum-Blasted	Plasma-Sprayed Microporous-Coated
S. aureus	97.9%	81.6%
S. epidermidis	93.4%	76.2%
E. coli	60.0%	100%

SEM

The biofilms were visualized after 24 h of culture using SEM. In Figures 6 and 7, the SEM images of the CB and PS discs, including uncoated and SML-coated discs for all

three strains, can be seen, respectively. On the uncoated discs, biofilms are clearly visible, whereas for the SML-coated discs, individual bacteria can be spotted.

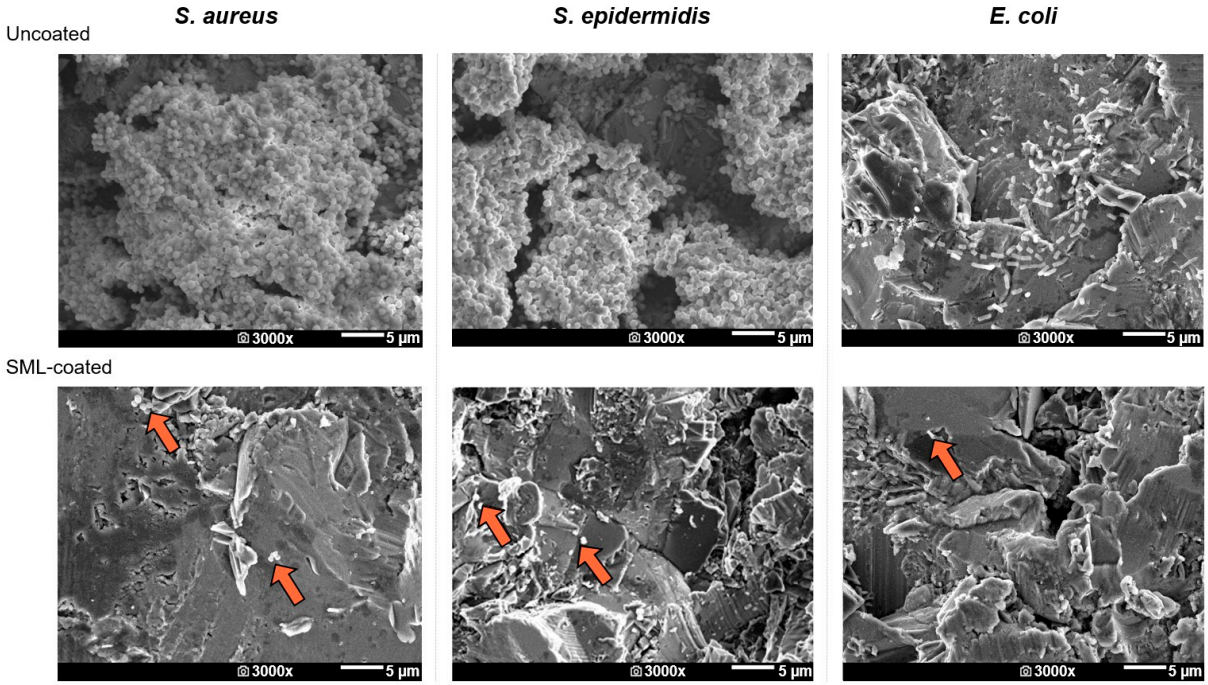

Figure 6. Corundum-blasted (CB) titanium discs after 24 h biofilm culture, with the uncoated discs (**upper row**) and SML-coated discs (**bottom row**) for all three bacterial strains divided per column. Orange arrows point out individual bacteria on the SML-coated discs. The magnification bars represent 5 µm.

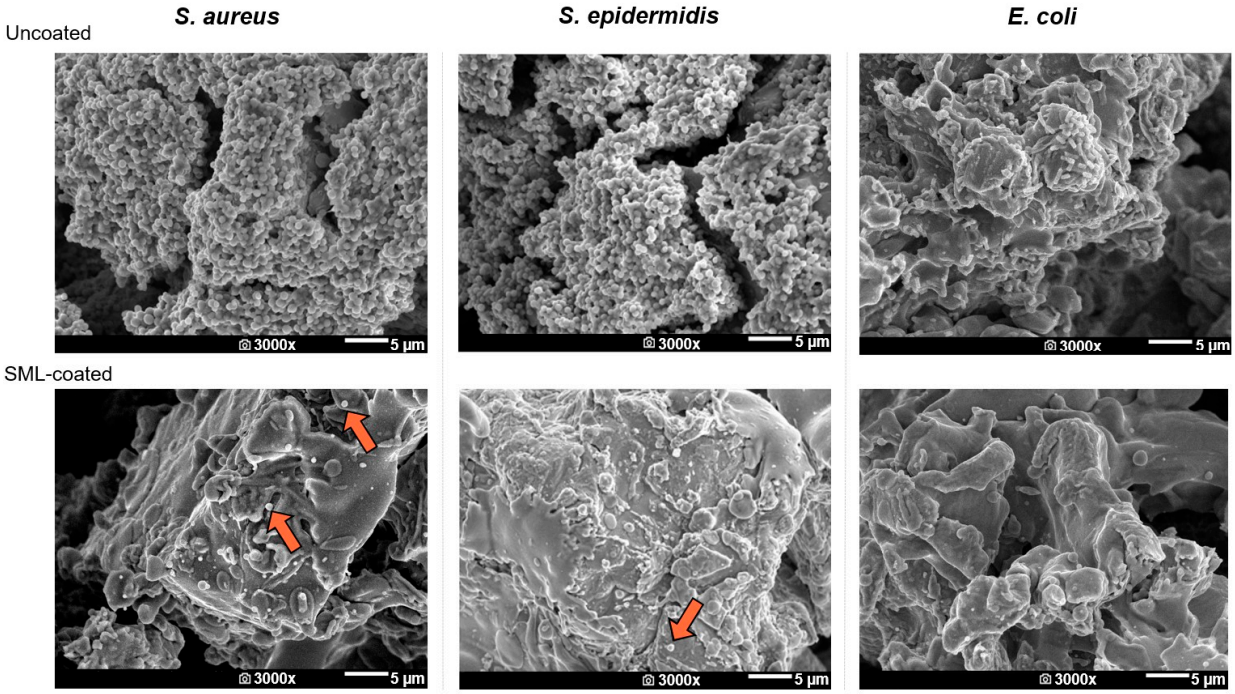

Figure 7. Plasma-sprayed microporous-coated (PS) titanium discs after 24 h biofilm culture, with the uncoated discs (**upper row**) and SML-coated discs (**bottom row**) for all three bacterial strains divided per column. Orange arrows point out individual bacteria on the SML-coated discs. The magnification bars represent 5 µm.

3.2.3. Effect of the SML Coating on Biofilm Dispersal

The daughter cells dispersed by the biofilms were cultured for 24 h, and daughter cell growth was assessed by measuring the OD_{600} at the start of culture and after 6 and 24 h. The OD_{600} values before the 24 h culture were comparable in all groups, and after 24 h, a saturated bacterial culture was present for all groups, as expected. In Table 4, the average ΔOD_{600} values (defined as $OD_{600,uncoated} - OD_{600,SML\text{-}coated}$) for each bacterial strain for both the CB and PS discs after 6 h of daughter cell cultivation are shown. For all groups, $\Delta OD_{600} > 0.3$ was found, indicating a reduction in proliferating daughter cells of 4-log scales when comparing daughter cell cultures from the uncoated and SML-coated discs.

Table 4. ΔOD_{600} values for each bacterial strain for both the corundum-blasted and plasma-sprayed microporous-coated titanium discs after 6 h of daughter cell cultivation.

Bacterial Strain	ΔOD_{600} (±SD)	
	Corundum-Blasted	Plasma-Sprayed Microporous-Coated
S. aureus	0.357 (±0.015)	0.366 (±0.002)
S. epidermidis	0.434 (±0.000)	0.449 (±0.001)
E. coli	0.496 (±0.001)	0.469 (±0.001)

4. Discussion

Biofilm formation is a major challenge in PJI treatment, and there is a critical need for preventative strategies for bacterial colonization and biofilm formation on orthopedic implants. Therefore, in this study, the antibacterial properties of the SML coating on two substrate materials common in orthopedic implants (CB and PS titanium) were investigated. It is known that surface properties, such as roughness or porosity, have a great effect on the ability of bacteria to adhere to a surface and grow a biofilm, and coating efficacy can depend on these properties. In addition, the effect of the SML coating on different phases in biofilm formation was assessed.

The antibacterial activity of the SML coating on the CB discs, according to test principles of ISO 22196, ASTM E2180-18, and JIS Z 2801 test standards, showed a >2-log reduction in CFUs on the sample surface for the SML-coated discs, as compared to the uncoated discs. Especially for the Gram-positive strains *S. aureus* and *S. epidermidis*, a strong effect was observed with a >3-log reduction in CFUs. The log reduction for *E. coli* was lower compared to the Gram-positive strains, which was to be expected as *E. coli* growth on the uncoated discs was higher than for the Gram-positive strains (dark green bars). In absolute numbers, a higher number of *E. coli* bacteria were killed by the coating than *S. aureus* or *S. epidermidis* bacteria. The efficacy of the coating can be explained by the release of a high enough concentration of silver ions from the metallic silver particles present in the coating. Silver ions have multiple mechanisms that are responsible for their antimicrobial properties. For example, silver ions bind to thiol groups in enzymes and proteins, damage the cell membrane, increase reactive oxygen species levels, and target the cell wall [51–54]. These interferences are responsible for cell disruption and interference in cellular processes. Bactericidal properties were found for all bacterial strains, as the levels of CFUs on the discs were lower after culture compared to the original inoculum. The antibacterial activity was also expressed in 'R', calculated according to the ISO 22196 standard. However, various descriptions for the interpretation of this value are present in the literature. When comparing the R-values reported in the literature, the R-value of 2.8 for *E. coli* is considered a significant antibacterial effect, and R-values of $R \geq 3.7$ for the Gram-positive strains are considered a strong antibacterial effect [55]. This is in line with log reductions in the viable bacteria found. A limitation of these test standards is that the PS discs were excluded due to their porosity.

Even though the strong antibacterial properties found indicate a reduction in biofilm formation on the SML-coated discs, a biofilm proliferation assay was performed to gain a deeper understanding of the prevention of biofilm formation and the antibacterial mecha-

nism of the coating. Coating efficacy after 1 h of initial bacterial adhesion, 24 h of biofilm cultivation (including the number of viable bacteria and biomass), and biofilm dispersal were assessed. The SML coating did not prevent bacterial adhesion after 1 h of incubation, which was expected due to the time required by the metallic silver present in the coating to be oxidized in a solution and subsequently, the silver ions that require time to diffuse to the coating surface. After 24 h of biofilm culture, a major decrease in viable bacteria on the sample surface was observed. Bacteriostatic and bactericidal properties were assessed, by observing whether the growth of adherent bacteria was inhibited or whether adherent bacteria were actively killed, respectively.

In the literature, the bacteriostatic and bactericidal properties of antimicrobial coatings are defined as the suppression of growth or the killing of bacteria in the original inoculum [47,56]. However, as culture media were refreshed after 1 h to include only adherent bacteria in the biofilm culture, the bacteria of the original inoculum that did not adhere to the surface were washed away. Therefore, we assess the bacteriostatic and bactericidal properties by comparing the CFU counts after 24 h of culture to the CFU counts after 1 h of adhesion, instead of comparing them to the original inoculum. Bactericidal properties were found for *S. aureus* and *S. epidermidis* on the CB discs, and the coating showed bacteriostatic properties in all other groups. However, in a biofilm culture without an intermediate washing step, the bacteriostatic and bactericidal properties can be assessed by comparing the CFU counts after culture with the original inoculum level. It is expected that in such an experimental setup, the bactericidal properties of the SML coating will also be found for more bacterial strains when coated on the PS discs. Given the fact that the SML coating showed bactericidal properties against *E. coli* in the antibacterial activity test and not in the biofilm proliferation assay, care must be taken when labeling antibacterial coatings as bacteriostatic or bactericidal, as the definition of these labels greatly depends on the washing steps used in the biofilm culture and the experimental set-up used.

The observed antibacterial properties highlight the significant value of the SML coating in clinical practice. When bacteria adhere to the implant surface, the SML-coated implant prevents the cascade of biofilm formation and maturation, which supports the host immune system to eliminate bacteria and win the race for the surface. The SML coating may even actively kill adherent bacteria [57]. However, an inoculum level of 10^6 CFUs/mL on a surface of 1.54 cm^2 is not realistic in a clinical scenario, as inoculum levels of 10^2–10^3 CFUs/mL are generally found on orthopedic implants in clinical practice [45,58–62]. With a lower inoculum level, active (or even complete) killing of the bacteria might occur. However, the large reductions in viable bacteria with the high inoculum used in this study emphasize the strength of the antibacterial properties of the SML coating. This is also supported by the decrease in daughter cells, dispersed by the biofilms. Daughter cell release was measured as the killing of mother cells on the surface by the SML coating, which is an important outcome as daughter cells are responsible for infection development [49,50]. In all groups, a large reduction in daughter cells was measured after 6 h of culture. This reduction in the growth activity of these offspring bacteria indicates a reduction in mother cells on the surface and therefore impaired dispersal of daughter cells by the biofilms grown on the surfaces [38,49].

Besides a reduction in viable bacteria and daughter cells released from the biofilms after 24 h of culture, a major reduction in biomass was found on the SML-coated discs. The CB discs showed lower absolute OD values than the PS discs. Safranin has been validated as a replacement for toxic crystal violet for staining biomass; however, it is known that safranin can yield lower OD values, indicating biofilm presence [48,63,64]. When looking at the CFU counts, more bacteria were present on the PS discs compared to the CB discs, except for *E. coli* growth on the PS discs. Even though these trends are consistent with the trends observed in the biomass measurements, it is unlikely that the number of viable bacteria explains the difference in biomass between the two types of discs. Matrix production might have been higher on the PS discs compared to the CB discs, induced by the structural changes and physiochemical factors between the two materials, leading to a

different bacterial response and activity when adhering to the surface [65]. For example, nutrient availability in the deeper pores of the PS discs can vary compared to the CB discs. However, the SEM images do not show differences in the biofilm matrix between the two materials, though only the superficial pores of the PS discs could be visualized. Also, it is known that SEM images often show poor-quality matrix structures, due to the fixation step when processing biofilms for SEM analysis [66]. Nevertheless, the SEM images were consistent with the CFU counts, showing a great reduction in biofilm formation.

This study is the first to investigate the efficacy of the SML coating with a Gram-negative bacterial strain. *E. coli* was chosen as the Gram-negative pathogen as this was prescribed by the ISO 22196 standard and together with *S. aureus* is a frequently used pathogen for in vitro efficacy tests of antibacterial coatings [45,67]. The Gram-negative bacteria showed different trends in sensitivity to the SML coating than the Gram-positive strains, as biofilm formation by the Gram-negative strain was more affected on the SML-PS discs, while the Gram-positive strains were more affected by the SML-CB discs. This is interesting, as the porous PS discs have a higher contact area for bacteria while the same quantity of SML coating, and thus, silver content was applied to these discs. Many factors may have contributed to this contradictory result for *E. coli* biofilm formation on two different surfaces. The susceptibility of bacteria to form a biofilm and the sensitivity of bacteria to an antibacterial compound depend greatly on their microenvironment and the availability of nutrients. As stated, the microenvironment of the bacteria on the PS discs can differ greatly from the microenvironment bacteria experience on the CB discs due to differences in porosity, roughness, and wettability. In future studies, an additional PJI-related Gram-negative bacterial species such as *Pseudomonas aeruginosa* should be included as well as a multispecies biofilm culture, as multispecies PJIs are frequent [68,69].

The current study presents a few other limitations and recommendations for future research. Firstly, a limitation of this study is the short biofilm culture of 24 h. The coating is expected to have a long-term antibacterial effect, so it would be interesting to include more time points with a longer biofilm culture period in a future study, including the CB and PS substrate surfaces. However, early intervention is crucial for surface-protecting coatings as it can then interfere with the proliferating germs on the implant surface. As the results show a positive rate between bacterial killing versus bacterial growth, no further biofilm maturation is expected. This is supported by a previous study, showing long-term coating efficacy on a stainless steel substrate [38]. Secondly, it would be recommended to include live/dead staining as a read-out parameter. Even though a strength of this study is the elaborate in vitro approach looking beyond CFU counts to assess the antimicrobial effect, including live/dead staining would give more support when assessing the bactericidal properties of the coating [37,38,67,70]. Lastly, general biomass stainings such as crystal violet and safranin are often used in biofilm research; however, molecular analysis of the contents of this biomass could lead to valuable insights regarding biofilm stability, metabolic state, and the antibacterial mechanism of anti-biofilm compounds [71]. Ongoing research is dedicated to investigating the ratio of biofilm components such as (e)DNA, carbohydrates, proteins, and lipids on biofilms formed on CB and PS discs with and without the SML coating. This will further elucidate the effect of surface roughness and porosity on biofilm formation and the mode of action of the SML coating.

5. Conclusions

In summary, the SML coating on CB and PS discs showed strong antibacterial properties. The coating did not prevent bacterial adhesion but inhibited biofilm growth by adherent bacteria and even killed Gram-positive bacteria when coated on CB discs. This study expands the understanding of the antibacterial mechanism of the SML coating and is the first to show coating efficacy with Gram-negative infection. Despite structural differences in substrate material such as roughness and porosity, the bacteria were highly susceptible to the antibacterial properties of the SML coating. The broad applicability and strong antibacterial properties found in this study with very low silver concentrations

present in the coating, leading to no cytotoxic effects as shown in previous studies, makes the SML coating a promising infection prophylaxis system for orthopedic applications. We conclude that this coating shows promising results to be effective in fighting PJI in a broad range of orthopedic implants.

Supplementary Materials: The supporting information can be downloaded at: https://www.mdpi.com/article/10.3390/coatings14020216/s1, Figure S1: SEM image of the cross-section of the SML coating; Figure S2: From left to right: Uncoated corundum-blasted titanium discs (Uncoated-CB), SML-coated corundum-blasted titanium discs (SML-CB), uncoated plasma-sprayed microporous-coated titanium discs (Uncoated-PS) and SML-coated plasma-sprayed microporous-coated titanium discs (SML-PS).

Author Contributions: Conceptualization, S.W.G.v.H., J.F., R.B., J.G. and J.J.C.A.; data curation, S.W.G.v.H. and L.C.W.P.; formal analysis, S.W.G.v.H.; investigation, S.W.G.v.H., J.L.v.A. and L.C.W.P.; methodology, S.W.G.v.H., J.F., R.B. and J.J.C.A.; resources, J.F. and R.B.; supervision, J.L.v.A.; visualization, S.W.G.v.H.; writing—original draft, S.W.G.v.H.; writing—review and editing, S.W.G.v.H., J.F., R.B., J.L.v.A., L.C.W.P., J.G. and J.J.C.A. All authors have read and agreed to the published version of the manuscript.

Funding: Maastricht University—This publication is part of the project Ambition, with project number NSP20–1-302. This collaboration project is co-funded by the PPP Allowance made available by Health-Holland, Top Sector Life Sciences & Health to ReumaNederland, in order to stimulate public–private partnerships. Aesculap AG—This publication is part of the project DARTBAC (with project number NWA.1292.19.354) of the research programme NWA-ORC which is (partly) financed by the Dutch Research Council (NWO).

Institutional Review Board Statement: Not applicable.

Informed Consent Statement: Not applicable.

Data Availability Statement: All data generated and analyzed during this study are included in this published article or depicted in the figures in this published article.

Acknowledgments: The author would like to thank Hans van Duimel for the assistance regarding the SEM analysis and Tim Welting for the discussions about the experimental set-up.

Conflicts of Interest: Authors Janine Fechter, Rainer Bargon were employed by the company Aesculap AG. Aesculap AG was involved as a consortium partner of the project DARTBAC (NWA.1292.19.354). The remaining authors declare that the research was conducted in the absence of any commercial or financial relationships that could be construed as a potential conflict of interest.

References

1. Natsuhara, K.M.; Shelton, T.J.; Meehan, J.P.; Lum, Z.C. Mortality During Total Hip Periprosthetic Joint Infection. *J. Arthroplast.* **2019**, *34*, S337–S342. [CrossRef]
2. Corvec, S.; Portillo, M.E.; Pasticci, B.M.; Borens, O.; Trampuz, A. Epidemiology and new developments in the diagnosis of prosthetic joint infection. *Int. J. Artif. Organs* **2012**, *35*, 923–934. [CrossRef] [PubMed]
3. Lentino, J.R. Prosthetic Joint Infections: Bane of Orthopedists, Challenge for Infectious Disease Specialists. *Clin. Pract.* **2003**, *36*, 1157–1161. [CrossRef] [PubMed]
4. Ong, K.L.; Kurtz, S.M.; Lau, E.; Bozic, K.J.; Berry, D.J.; Parvizi, J. Prosthetic joint infection risk after total hip arthroplasty in the Medicare population. *J. Arthroplast.* **2009**, *24*, 105–109. [CrossRef] [PubMed]
5. Zeng, Z.J.; Yao, F.M.; He, W.; Wei, Q.S.; He, M.C. Incidence of periprosthetic joint infection after primary total hip arthroplasty is underestimated: A synthesis of meta-analysis and bibliometric analysis. *J. Orthop. Surg. Res.* **2023**, *18*, 610. [CrossRef] [PubMed]
6. Huotari, K.; Lyytikainen, O.; Ollgren, J.; Virtanen, M.J.; Seitsalo, S.; Palonen, R.; Rantanen, P.; Hospital Infection Surveillance, T. Disease burden of prosthetic joint infections after hip and knee joint replacement in Finland during 1999-2004: Capture-recapture estimation. *J. Hosp. Infect.* **2010**, *75*, 205–208. [CrossRef] [PubMed]
7. Kurtz, S.M.; Ong, K.L.; Lau, E.; Bozic, K.J.; Berry, D.; Parvizi, J. Prosthetic joint infection risk after TKA in the Medicare population. *Clin. Orthop. Relat. Res.* **2010**, *468*, 52–56. [CrossRef] [PubMed]
8. Day, C.W.; Costi, K.; Pannach, S.; Atkins, G.J.; Hofstaetter, J.G.; Callary, S.A.; Nelson, R.; Howie, D.W.; Solomon, L.B. Long-Term Outcomes of Staged Revision Surgery for Chronic Periprosthetic Joint Infection of Total Hip Arthroplasty. *J. Clin. Med.* **2021**, *11*, 122. [CrossRef] [PubMed]

9. Patel, I.; Nham, F.; Zalikha, A.K.; El-Othmani, M.M. Epidemiology of total hip arthroplasty: Demographics, comorbidities and outcomes. *Arthroplasty* **2023**, *5*, 2. [CrossRef]
10. Nham, F.H.; Patel, I.; Zalikha, A.K.; El-Othmani, M.M. Epidemiology of primary and revision total knee arthroplasty: Analysis of demographics, comorbidities and outcomes from the national inpatient sample. *Arthroplasty* **2023**, *5*, 18. [CrossRef]
11. Bozic, K.J.; Kurtz, S.M.; Lau, E.; Ong, K.; Chiu, V.; Vail, T.P.; Rubash, H.E.; Berry, D.J. The Epidemiology of Revision Total Knee Arthroplasty in the United States. *Clin. Orthop. Relat. Res.* **2010**, *468*, 45–51. [CrossRef]
12. Sloan, M.; Premkumar, A.; Sheth, N.P. Projected Volume of Primary Total Joint Arthroplasty in the U.S., 2014 to 2030. *J. Bone Jt. Surg. Am.* **2018**, *100*, 1455–1460. [CrossRef] [PubMed]
13. Izakovicova, P.; Borens, O.; Trampuz, A. Periprosthetic joint infection: Current concepts and outlook. *EFORT Open Rev.* **2019**, *4*, 482–494. [CrossRef]
14. Kurtz, S.; Ong, K.; Lau, E.; Mowat, F.; Halpern, M. Projections of primary and revision hip and knee arthroplasty in the United States from 2005 to 2030. *J. Bone Jt. Surg. Am.* **2007**, *89*, 780–785. [CrossRef]
15. Ferguson, R.J.; Palmer, A.J.; Taylor, A.; Porter, M.L.; Malchau, H.; Glyn-Jones, S. Hip replacement. *Lancet* **2018**, *392*, 1662–1671. [CrossRef] [PubMed]
16. Ventola, C.L. The Antibiotic Resistance Crisis. *Pharm. Ther.* **2015**, *40*, 277–283.
17. Rottier, W.; Seidelman, J.; Wouthuyzen-Bakker, M. Antimicrobial treatment of patients with a periprosthetic joint infection: Basic principles. *Arthroplasty* **2023**, *5*, 10. [CrossRef] [PubMed]
18. Baddour, L.M.; Chen, A.F. *Prosthetic Joint Infection: Treatment*; UpToDate: Waltham, MA, USA, 2023.
19. Anagnostakos, K.; Schmitt, C. Can periprosthetic hip joint infections be successfully managed by debridement and prosthesis retention? *World J. Orthop.* **2014**, *5*, 218–224. [CrossRef]
20. Premkumar, A.; Kolin, D.A.; Farley, K.X.; Wilson, J.M.; McLawhorn, A.S.; Cross, M.B.; Sculco, P.K. Projected Economic Burden of Periprosthetic Joint Infection of the Hip and Knee in the United States. *J. Arthroplast.* **2021**, *36*, 1484–1489. [CrossRef]
21. Scheper, H.; Gerritsen, L.M.; Pijls, B.G.; Van Asten, S.A.; Visser, L.G.; De Boer, M.G.J. Outcome of Debridement, Antibiotics, and Implant Retention for Staphylococcal Hip and Knee Prosthetic Joint Infections, Focused on Rifampicin Use: A Systematic Review and Meta-Analysis. *Open Forum Infect. Dis.* **2021**, *8*, ofab298. [CrossRef]
22. Gbejuade, H.O.; Lovering, A.M.; Webb, J.C. The role of microbial biofilms in prosthetic joint infections. *Acta Orthop.* **2015**, *86*, 147–158. [CrossRef]
23. Costerton, J.W.; Lewandowski, Z. Microbial biofilm. *Annu. Rev. Microbial.* **1995**, *49*, 711–745. [CrossRef]
24. Arts, J.; Geurts, J. *Management of Periprosthetic Joint Infections (PJIs)*; Springer: Berlin/Heidelberg, Germany, 2017; pp. 1–306.
25. Kostakioti, M.; Hadjifrangiskou, M.; Hultgren, S.J. Bacterial biofilms: Development, dispersal, and therapeutic strategies in the dawn of the postantibiotic era. *Cold Spring Harb. Perspect. Med.* **2013**, *3*, a010306. [CrossRef]
26. Lora-Tamayo, J.; Murillo, O.; Iribarren, J.A.; Soriano, A.; Sanchez-Somolinos, M.; Baraia-Etxaburu, J.M.; Rico, A.; Palomino, J.; Rodriguez-Pardo, D.; Horcajada, J.P.; et al. A large multicenter study of methicillin-susceptible and methicillin-resistant Staphylococcus aureus prosthetic joint infections managed with implant retention. *Clin. Infect. Dis.* **2013**, *56*, 182–194. [CrossRef]
27. Casenaz, A.; Piroth, L.; Labattut, L.; Sixt, T.; Magallon, A.; Guilloteau, A.; Neuwirth, C.; Amoureux, L. Epidemiology and antibiotic resistance of prosthetic joint infections according to time of occurrence, a 10-year study. *J. Infect.* **2022**, *85*, 492–498. [CrossRef]
28. Hays, M.R.; Kildow, B.J.; Hartman, C.W.; Lyden, E.R.; Springer, B.D.; Fehring, T.K.; Garvin, K.L. Increased Incidence of Methicillin-Resistant Staphylococcus aureus in Knee and Hip Prosthetic Joint Infection. *J. Arthroplast.* **2023**, *38*, S326–S330. [CrossRef]
29. Svensson Malchau, K.; Tillander, J.; Zaborowska, M.; Hoffman, M.; Lasa, I.; Thomsen, P.; Malchau, H.; Rolfson, O.; Trobos, M. Biofilm properties in relation to treatment outcome in patients with first-time periprosthetic hip or knee joint infection. *J. Orthop. Transl.* **2021**, *30*, 31–40. [CrossRef] [PubMed]
30. Li, H.; Wang, D.; Zhang, W.; Xu, G.; Xu, C.; Liu, W.; Li, J. Potential side effects of antibacterial coatings in orthopaedic implants: A systematic review of clinical studies. *Front. Bioeng. Biotechnol.* **2023**, *11*, 1111386. [CrossRef] [PubMed]
31. Yin, I.X.; Zhang, J.; Zhao, I.S.; Mei, M.L.; Li, Q.; Chu, C.H. The Antibacterial Mechanism of Silver Nanoparticles and Its Application in Dentistry. *Int. J. Nanomed.* **2020**, *15*, 2555–2562. [CrossRef] [PubMed]
32. Alt, V. Antimicrobial coated implants in trauma and orthopaedics—A clinical review and risk-bene fi t analysis. *Inj. Int. J. Care Inj.* **2017**, *48*, 599–607. [CrossRef] [PubMed]
33. Rathbone, C.R.; Cross, J.D.; Brown, K.V.; Murray, C.K.; Wenke, J.C. Effect of various concentrations of antibiotics on osteogenic cell viability and activity. *J. Orthop. Res.* **2011**, *29*, 1070–1074. [CrossRef]
34. Pauksch, L.; Hartmann, S.; Rohnke, M.; Szalay, G.; Alt, V.; Schnettler, R.; Lips, K.S. Biocompatibility of silver nanoparticles and silver ions in primary human mesenchymal stem cells and osteoblasts. *Acta Biomater.* **2014**, *10*, 439–449. [CrossRef]
35. Alt, V.; Chen, A.F. Antimicrobial coatings for orthopaedic implants—Ready for use? *J. Bone Jt. Infect.* **2020**, *5*, 125–127. [CrossRef]
36. Malhotra, R.; Dhawan, B.; Garg, B.; Shankar, V.; Nag, T.C. A Comparison of Bacterial Adhesion and Biofilm Formation on Commonly Used Orthopaedic Metal Implant Materials: An In vitro Study. *Indian J. Orthop.* **2019**, *53*, 148–153. [CrossRef] [PubMed]
37. Fabritius, M.; Al-Munajjed, A.A.; Freytag, C.; Jülke, H.; Zehe, M.; Lemarchand, T.; Arts, J.J.; Schumann, D.; Alt, V.; Sternberg, K. Antimicrobial silver multilayer coating for prevention of bacterial colonization of orthopedic implants. *Materials* **2020**, *13*, 1415. [CrossRef] [PubMed]

38. Khalilpour, P.; Lampe, K.; Wagener, M.; Stigler, B.; Heiss, C.; Ullrich, M.S.; Domann, E.; Schnettler, R.; Alt, V. Ag/SiOxCy plasma polymer coating for antimicrobial protection of fracture fixation devices. *J. Biomed. Mater. Res.* **2010**, *94B*, 196–202. [CrossRef]
39. Azab, M.A.; Allen, M.J.; Daniels, J.B. Evaluation of a silver-impregnated coating to inhibit colonization of orthopaedic implants by biofilm forming methicillin-resistant *Staphylococcus pseudintermedius*. *Vet. Comp. Orthop. Traumatol.* **2016**, *29*, 347–350. [CrossRef]
40. Stein, S.; Kruck, L.; Warnecke, D.; Seitz, A.; Durselen, L.; Ignatios, A. Osseointegration of titanium implants with a novel silver coating under dynamic loading. *Eur. Cells Mater.* **2020**, *39*, 249–259. [CrossRef] [PubMed]
41. Alt, V.; Heiss, C.; Rupp, M. Treatment of a Recurrent Periprosthetic Joint Infection with an Intramedullary Knee Arthrodesis System with Low-Amount Metallic Silver Coating. *J. Bone Jt. Infect.* **2019**, *4*, 111–114. [CrossRef]
42. Zheng, S.; Bawazir, M.; Dhall, A.; Kim, H.-e.; He, L.; Heo, J.; Hwang, G. Implication of Surface Properties, Bacterial Motility, and Hydrodynamic Conditions on Bacterial Surface Sensing and Their Initial Adhesion. *Front. Bioeng. Biotechnol.* **2021**, *9*, 643722. [CrossRef]
43. *ISO 22196:2011(E)*; Measurement of Antibacterial Activity on Plastics and Other Non-Porous Surfaces. ISO: Geneva, Switzerland, 2011.
44. *ASTM E2180-18*; Standard Test Method for Determining the Activity of Incorporated Antimicrobial Agent(s) in Polymeric or Hydrophobic Materials. American Society for Testing and Materials (ASTM): West Conshohocken, PA, USA, 2018.
45. Sjollema, J.; Zaat, S.A.J.; Fontaine, V.; Ramstedt, M.; Luginbuehl, R.; Thevissen, K.; Li, J.; van der Mei, H.C.; Busscher, H.J. In vitro methods for the evaluation of antimicrobial surface designs. *Acta Biomater.* **2018**, *70*, 12–24. [CrossRef]
46. Zhang, X.; Ma, Y.F.; Wang, L.; Jiang, N.; Qin, C.H.; Hu, Y.J.; Yu, B. A rabbit model of implant-related osteomyelitis inoculated with biofilm after open femoral fracture. *Exp. Ther. Med.* **2017**, *14*, 4995–5001. [CrossRef] [PubMed]
47. Bernatova, S.; Samek, O.; Pilat, Z.; Sery, M.; Jezek, J.; Jakl, P.; Siler, M.; Krzyzanek, V.; Zemanek, P.; Hola, V.; et al. Following the mechanisms of bacteriostatic versus bactericidal action using Raman spectroscopy. *Molecules* **2013**, *18*, 13188–13199. [CrossRef] [PubMed]
48. Ommen, P.; Zobek, N.; Meyer, R.L. Quantification of biofilm biomass by staining: Non-toxic safranin can replace the popular crystal violet. *J. Microbiol. Methods* **2017**, *141*, 87–89. [CrossRef] [PubMed]
49. Bruenke, J.; Roschke, I.; Agarwal, S.; Riemann, T.; Greiner, A. Quantitative Comparison of the Antimicrobial Efficiency of Leaching versus Nonleaching Polymer Materials. *Macromol. Biosci.* **2016**, *16*, 647–654. [CrossRef] [PubMed]
50. Bechert, T.; Steinrücke, P.; Guggenbichler, J.P. A new method for screening anti-infective biomaterials. *Nat. Med.* **2000**, *6*, 1053–1056. [CrossRef]
51. Schreurs, W.J.A.; Rosenberg, H. Effect of Silver Ions on Transport and Retention of Phosphate by Escherichia coli. *J. Bacteriol.* **1982**, *152*, 7–13. [CrossRef]
52. Thurman, R.B.; Gerba, C.P.; Bitton, G. The molecular mechanisms of copper and silver ion disinfection of bacteria and viruses. *Crit. Rev. Environ. Control* **1989**, *18*, 295–315. [CrossRef]
53. Dakal, T.C.; Kumar, A.; Majumdar, R.S.; Yadav, V. Mechanistic Basis of Antimicrobial Actions of Silver Nanoparticles. *Front. Microbiol.* **2016**, *7*, 1831. [CrossRef]
54. Jung, W.K.; Koo, H.C.; Kim, K.W.; Shin, S.; Kim, S.H.; Park, Y.H. Antibacterial activity and mechanism of action of the silver ion in Staphylococcus aureus and Escherichia coli. *Appl. Environ. Microbiol.* **2008**, *74*, 2171–2178. [CrossRef]
55. Wiegand, C.; Völpel, A.; Ewald, A.; Remesch, M.; Kuever, J.; Bauer, J.; Griesheim, S.; Hauser, C.; Thielmann, J.; Tonndorf-Martini, S.; et al. Critical physiological factors influencing the outcome of antimicrobial testing according to ISO 22196/JIS Z 2801. *PLoS ONE* **2018**, *13*, e0194339. [CrossRef] [PubMed]
56. Pankey, G.A.; Sabath, L.D. Clinical Relevance of Bacteriostatic versus Bactericidal Mechanisms of Action in the Treatment of GramPositive Bacterial Infections. *Clin. Infect. Dis.* **2004**, *38*, 864–870. [CrossRef]
57. Subbiahdoss, G.; Kuijer, R.; Grijpma, D.W.; van der Mei, H.C.; Busscher, H.J. Microbial biofilm growth vs. tissue integration: "the race for the surface" experimentally studied. *Acta Biomater.* **2009**, *5*, 1399–1404. [CrossRef]
58. Reizner, W.; Hunter, J.G.; O'Malley, N.T.; Southgate, R.D.; Schwarz, E.M.; Kates, S.L. A systematic review of animal models for Staphylococcus aureus osteomyelitis. *Eur. Cell Mater.* **2015**, *27*, 196–212. [CrossRef]
59. Moriarty, T.F.; Debefve, L.; Boure, L.; Campoccia, D.; Schlegel, U.; Richards, R.G. Influence of material and microtopography on the development of local infection in vivo: Experimental investigation in rabbits. *Int. J. Artif. Organs* **2009**, *32*, 663–670. [CrossRef]
60. Moriarty, T.F.; Campoccia, D.; Nees, S.K.; Boure, L.P.; Richards, R.G. In vivo evaluation of the effect of intramedullary nail microtopography on the development of local infection in rabbits. *Int. J. Artif. Organs* **2010**, *33*, 667–675. [CrossRef]
61. Elek, S.D.; Conen, P.E. The virulence of staphylococcus pyogenes for man. A study of the problems of wound infection. *Br. J. Exp. Pathol.* **1957**, *38*, 573–586. [PubMed]
62. Trampuz, A.; Piper, K.E.; Jacobson, M.J.; Hanssen, A.D.; Unni, K.K.; Osmon, D.R.; NMandrekar, J.N.; Cockerill, F.R.; Steckelberg, J.M.; Greenleaf, J.F.; et al. Sonication of Removed Hip and Knee Prostheses for Diagnosis of Infection. *N. Engl. J. Med.* **2007**, *357*, 654–663. [CrossRef] [PubMed]
63. Standar, K.; Kreikemeyer, B.; Redanz, S.; Munter, W.L.; Laue, M.; Podbielski, A. Setup of an in vitro test system for basic studies on biofilm behavior of mixed-species cultures with dental and periodontal pathogens. *PLoS ONE* **2010**, *5*, e13135. [CrossRef]
64. Stiefel, P.; Rosenberg, U.; Schneider, J.; Mauerhofer, S.; Maniura-Weber, K.; Ren, Q. Is biofilm removal properly assessed? Comparison of different quantification methods in a 96-well plate system. *Appl. Microbiol. Biotechnol.* **2016**, *100*, 4135–4145. [CrossRef]

65. Oh, J.K.; Yegin, Y.; Yang, F.; Zhang, M.; Li, J.; Huang, S.; Verkhoturov, S.V.; Schweikert, E.A.; Perez-Lewis, K.; Scholar, E.A.; et al. The influence of surface chemistry on the kinetics and thermodynamics of bacterial adhesion. *Sci. Rep.* **2018**, *8*, 17247. [CrossRef]
66. Dassanayake, R.P.; Falkenberg, S.M.; Stasko, J.A.; Shircliff, A.L.; Lippolis, J.D.; Briggs, R.E. Identification of a reliable fixative solution to preserve the complex architecture of bacterial biofilms for scanning electron microscopy evaluation. *PLoS ONE* **2020**, *15*, e0233973. [CrossRef]
67. Cunliffe, A.J.; Askew, P.D.; Stephan, I.; Iredale, G.; Cosemans, P.; Simmons, L.M.; Verran, J.; Redfern, J. How do we determine the efficacy of an antibacterial surface? A review of standardised antibacterial material testing methods. *Antibiotics* **2021**, *10*, 1069. [CrossRef]
68. Zmistowski, B.; Fedorka, C.J.; Sheehan, E.; Deirmengian, G.; Austin, M.S.; Parvizi, J. Prosthetic joint infection caused by gram-negative organisms. *J. Arthroplast.* **2011**, *26*, 104–108. [CrossRef]
69. Perni, S.; Bojan, B.; Prokopovich, P. A retrospective study of risk factors, causative micro-organisms and healthcare resources consumption associated with prosthetic joint infections (PJI) using the Clinical Practice Research Datalink (CPRD) Aurum database. *PLoS ONE* **2023**, *18*, e0282709. [CrossRef] [PubMed]
70. Robertson, J.; McGoverin, C.; Vanholsbeeck, F.; Swift, S. Optimisation of the Protocol for the LIVE/DEAD((R)) BacLight(TM) Bacterial Viability Kit for Rapid Determination of Bacterial Load. *Front. Microbiol.* **2019**, *10*, 801. [CrossRef] [PubMed]
71. Wilson, C.; Lukowics, R.; Merchant, S.; Valquier-Flynn, H.; Caballero, J.; Sandoval, J.; Okuom, M.; Huber, C.; Durham Brooks, T.; Wilson, E.; et al. Quantitative and Qualitative Assessment Methods for Biofilm Growth: A Mini-review. *Res. Rev. J. Eng. Technol.* **2017**, *6*, 1–25.